STATUS OF INSERTION DEVICES AT TAIWAN PHOTON SOURCE

T.Y. Chung†, J.C. Huang, J.C. Jan, M.S. Chiu, F.H. Tseng, Y.C. Liu, C.C. Kuo, C.H. Chang, C.K. Yang, C.H. Chang, and C.S. Hwang
National Synchrotron Radiation Research Center, Hsinchu, Taiwan

Abstract

The storage ring of Taiwan Photon Source (TPS) has eighteen short straight sections (length 7 m) and six long straight sections (length 12 m). In phase I, three elliptically polarized undulators of type APPLE II and seven in-vacuum undulators, which included four in-vacuum undulators and two elliptically polarized undulators in three double mini-β_y sections, were installed. Commissioning of the insertion devices began in 2015 November. The influence of insertion devices on the electron beam and the results after compensation are presented. Problems during the commissioning induced by the electron beam and by radiation, and their solutions, are also explained. For insertion devices in phase II and for devices developed in TPS, the preliminary designs are presented herein, to cover from the VUV to the hard X-ray region.

INTRODUCTION

TPS is a new, third-generation, 3-GeV synchrotron radiation facility that was commissioned by 2014 December [1]. The facility plans to have many and varied insertion devices (ID) that will serve for user beamlines in scientific applications of radiation in the VUV, soft and hard X-ray ranges. According to the requirements of users, all phase-I ID are undulators. Three elliptically polarized undulators (EPU) of type APPLE II are dedicated for radiation in the soft X-ray range, with variable polarization. Seven planar in-vacuum undulators (IU) are used for hard X-rays; among them, one in-vacuum tapered undulator (IUT) serves to increase the photon band width. Table 1 lists the characteristics of the ID in phase I.

Table 1: TPS Phase-I ID Parameters

	EPU48	EPU46	IU22/IUT22	IU22
photon energy (keV)	0.22-2	0.28-2	1.8-20	1.84-20
type	APPLEII	APPLEII	Planar In-vacuum	Planar In-vacuum
deflection parameter K_y/K_x	3.74/2.46	3.35/2.23	1.52	1.49
period length (mm)	48	46	22	22
number of periods	68	82	140	95
total length (m)	3.2	3.8	3.1	2.1
number	2	1	4/1	2
range of magnet gap (mm)	13-120	14-110	7-40	7-40

† email address: chung.albert@nsrrc.org.tw

EPU

A tandem EPU48 and a phase shifter between them were installed in double mini-β_y sections to increase the angular density of flux, as shown in Fig. 1(a). Both EPU were designed and constructed in National Synchrotron Radiation Research Center (NSRRC). Many techniques and much knowledge to build EPU were developed, such as to control accumulated mechanical error, for mechanical assembly, and for magnet sorting and shimming algorithms [2].

Figure 1: (a) Installation of two EPU48 in the TPS storage ring. (b) Protection of a linear encoder with a lead shielding box.

During the early stage of commissioning, soft errors of linear encoders occurred frequently, especially for phase movement. These errors are attributed to radiation damage that arose from an unstable orbit of the electron beam. To decrease these incidents [3], linear encoders of the gap and the phase movement were housed in boxes with lead shielding of thickness about 10 mm, as shown in Fig. 1(b).

The influence of ID on the electron beam was measured and compensated based on beam-based measurements (BBM) [4]. The residual field integral from an ID was measured in both planes according to an analysis of the closed-orbit distortions (COD) and compared with the results in the magnetic measurement facility (MMF). Figure 2 shows the consistent behaviour of both results in the field integrals dependent on the gap and phase. The discrepancy under 20 G cm might arise from a variation of the surrounding field and a contribution from the second-order effect due to a slight alignment error.

The tune shifts observed after a careful treatment of the first-order effect in the MMF were attributed to a second-order effect. Because of an inherently poor roll-off of the APPLE II in a vertical-polarization mode (P_{24}), the evident horizontal defocusing and vertical focusing behaviours were predicted according to the second-order effect. Tune shifts dependent on the gap in three modes of polarization behaved consistent with expectations of the second-order effect, as shown in Fig. 3. The present

strategy for compensation is to use pairs of quadrupole magnets nearby the EPU. Further study of high-order multipole effects is in progress.

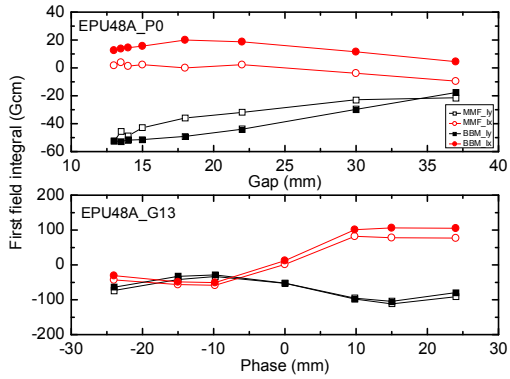

Figure 2: Top: First field integral of EPU48A, dependent on the gap, at a horizontal polarization (P_0). Bottom: the first field integral of EPU48A, dependent on the phase, at the minimum gap 13 mm; magnetic measurements (open) and beam measurements (solid). The square and circles indicate the vertical and horizontal field integrals, respectively.

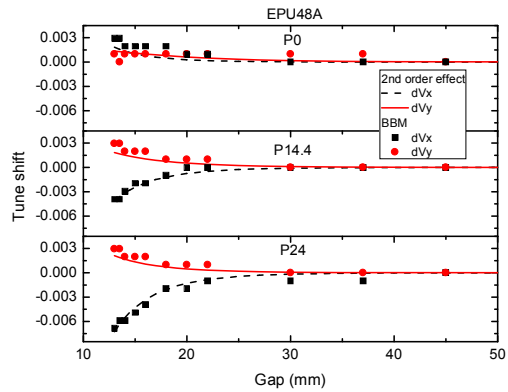

Figure 3: Gap-dependent tune shift measured in both planes at horizontal (P_0), circular ($P_{14.4}$) and vertical (P_{24}) polarizations. Prediction from calculation of second-order effects: horizontal (dashed line), and vertical (solid line) tune shifts. Results from measurements based on beams: horizontal (squares) and vertical (circles) tune shifts.

At an ID installed upstream of a long straight section in TPS, there is a great risk of heating of the vacuum chambers by synchrotron radiation. A small gap in the vacuum chamber along the path of the photon beam limits the maximum allowed horizontal deflection parameter (K_x), resulting in a minimum photon energy of radiation with vertical and circular polarizations. Figure 4 shows a spatial power density of an EPU48 at a minimum gap 13 mm for circular polarization. The original vacuum chamber of a bending magnet in the path of the photon beam had a small gap, 9 mm. The range of the angle of divergence from the middle of the EPU to the 9-mm gap in the vacuum section is indicated by the window in Fig.4. The peak power of synchrotron radiation with circular polarization from the upstream EPU would have struck the 9-mm gap in the vacuum section, resulting in a serious heat load. During the long shutdown in 2016 spring, the gap of the vacuum chamber was increased to 18 mm; the allowable maximum K_x is thus 3.5 [5].

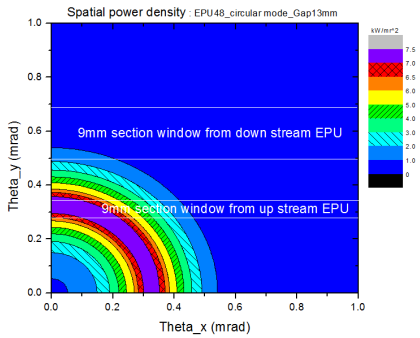

Figure 4: Spatial power density of an EPU48 at the minimum gap, 13 mm, in the circular polarization mode.

Parallel EPU and Knot-APPLE

For phase-II ID requirements of a NanoARPES user, an EPU installed in one location must deliver photons of energy less than 20 eV and also cover the flux density with photon energy up to 400 eV. The best solution is to choose two period lengths of EPU, arranged in parallel, of which each can have the maximum number of periods. A preliminary design of this parallel EPU, which will be installed in a short straight section, has period lengths 100 and 50 mm, both of total length 4 m. For VUV photons required to have energy less than 5 eV, an ID must have a large deflection parameter, resulting in a large heat load on the beamline optics. In our preliminary design, an undulator of type Knot-APPLE can decrease the power efficiently from 2.2 to 0.09 kW for length 4 m [6]. Further investigation is in progress.

IU

Although seven IU22 were constructed by Hitachi-Metal, NSRRC modified and improved several parts of these IU22, including designing a RF transition taper to increase the capability of cooling, changing the method of clamping a copper-nickel foil to the surface to prevent the creation of a bump, and designing a pole piece to improve roll-off [7]. As IU share the vacuum with the storage ring, baking is necessary. The total duration of baking was 60 h, of which the first 10 h involved raising the temperature, the next 40 h had the temperature in a stable state, and the last 10 h were for decreasing the temperature. For seven IU22, an average pressure was 9.8 $\times 10^{-9}$ Pa during 30 days after baking.

One accident related to a water-cooling pipe of a RF transition taper that occurred during the ID baking; a serious vacuum leakage was detected,as shown in Fig. 5(a) A rigorous analysis (using an electron probe X-ray analyser, a SEM and an ion chromatograph) indicated a possible cause, namely nitric acid (HNO_3) that remained on the copper surface after cleaning. The evacuation of air caused water to evaporate and the concentration of HNO_3

ISBN 978-3-95450-147-2

to increase. Concentrated HNO_3 caused erosion of the copper pipe and the reaction with copper to produce $Cu(NO_3)_2$. Baking at high temperature converted the $Cu(NO_3)_2$ into CuO. The evidence shows that the vacuum leakage was produced from an oxidized surface of the cooling pipe. The accident was quickly rectified on replacing the cooling-water pipe, and the IU was baked once more.

After the orbit of the electron beam and the double mini-β_y lattice were optimized, the multipole errors arising from the IU were measured and corrected. The special concerns for the operation of a mini-gap IU are the decreased life time of the beam and the injection efficiency. When a feed-forward table of steering magnets is applied to correct the residual field integral, each IU22 was closed to test the injection efficiency; there was no obvious change in the IU operation. When seven IU were near the minimum gap, the vertical and horizontal tune shift changes were 0.01 and 0, respectively.

To utilize a mini-gap IU, two tandems IU22 were installed in two double mini-β_y sections to prevent an obstacle from the vertical betatron function at the end of an IU. Because of the lattice design, an IU22 was intended to have a minimum gap 5 mm. Figure 5(b) shows an installation of an IU22 in the TPS storage ring. Not only beam cleaning but also the heat load on the copper-nickel foil must be considered when an IU operates at a large beam current and a small gap. The radiation or image current, or both, can provide a large heat load on the foil, resulting in a melting damage to the foil. In the case of a tandem ID, the radiation from the upstream bending magnet and the ID was strictly aligned in the same horizontal plane.

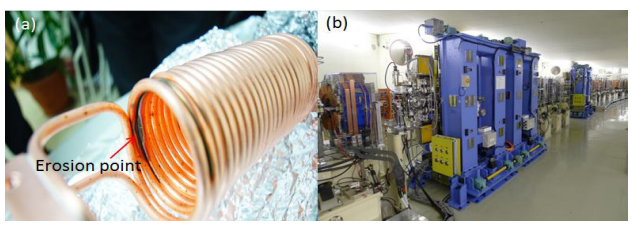

Figure 5: (a) Erosion to a water-cooling pipe of a RF transition taper. (b) Installation of two IU22 in the TPS storage ring.

Cryogenic Undulator

To increase the brilliance in the hard X-ray region, a period of small length for an undulator to increase the number of periods is necessary. Cooling the magnet blocks is hence one solution to increase the magnetic field and to maintain a tunability of an undulator with a small period. NSRRC cooperates with Hitachi-Metal to develop a cryogenic undulator (CU). According to a preliminary design, the major parameters are period length 15 mm, magnetic material PrFeB, and operating temperature 77~100 K [8]. Based on these parameters, the brilliance is shown in Fig. 6. A CU15 can provide a light source of brilliance greater than the present IU22 undulators used in TPS beamlines of phase I. At photon energy 10 keV, the brilliance of CU15-1 m, -2 m and -3 m is about 135, 159 and 234 % of IU22-3 m, respectively.

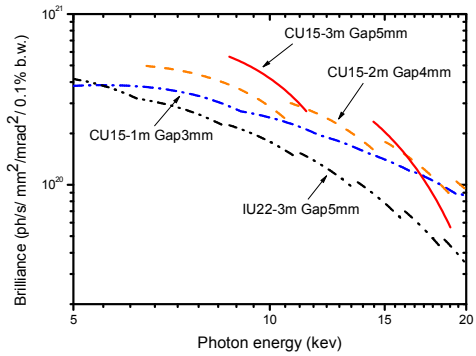

Figure 6: Comparison of brilliance performance of CU15-3m CU15-2m, CU15-1m and IU22-3m.

MULTIPOLE WIGGLER

To serve a user of a wiggler who requires a photon energy in the range 6-18 keV, a hybrid-type multipole wiggler (MPW) was proposed, instead of using a superconducting technique, which requires heavy maintenance and running costs [9]. In our design, the MPW is an outside-vacuum type and is optimized to have a short period, resulting in an intense angular density of flux. According to a preliminary design, the major parameters are operation gap 14 mm, period length 100 mm, and magnetic field 1.8 T.

CONCLUSION

To serve scientific applications, ten undulators were installed and are being commissioned in phase I. The ID-induced perturbations of the linear optics were compensated. During the commissioning, the damage from synchrotron radiation is a major issue. Several projects for phase-II ID or requirements of users are in progress, including the development of a Knot-APPLE for VUV, a cryogenic undulator for hard X-rays, and a hybrid-type multipole wiggler.

REFERENCES

[1] C.C. Kuo, *et al.* "Commissioning of the Taiwan Photon Source" IPAC, 1314–1318 (2015).
[2] T.Y. Chung, *et al.* Synchrotron Radiation News 28, 29 (2015).
[3] C.H. Huang, *et al.* "Preliminary Beam-loss Study of TPS during Beam Commissioning", these proceedings.
[4] M.S. Chiu, *et al.* "The commissioning of phase-I insertion devices in TPS", these proceedings.
[5] I.C. Sheng, *et al.* "Chamber Upgrade for EPU48 in TPS", these proceedings.
[6] S. Sasaki, *et al.* "Design study of Knot-APPLE undulator for PES-beamline at SSRF", PAC, 1043–1045 (2013).
[7] J.C. Huang, *et al.* "Challenge of in-vacuum and cryogenic undulators", these proceedings.
[8] J.C. Huang, *et al.* "Magnetic Circuit Design of a Cryogenic Undulator in Taiwan Photon Source", SRI (2015).
[9] J.C. Jan, *et al.* "Optimization of a multipole wiggler for TPS", these proceedings.